**Volume 4, No. 8 August 2026**
p-ISSN3032-3037| e-ISSN 3031-5786

ADVANCES IN SOCIAL HUMANITIES RESEARCH

# Feasibility Evaluation of Repurposing Subsea Gas Pipelines i the Floating Storage and Regasification Unit System in West Java – Muara Karang Onshore Receiving Facility for Hydrogen Blending Transportation

**Yurnaldi Akbar*, Suwarno, Witantyo**
Institut Teknologi Sepuluh November, Indonesia
Email: 6007241064@student.its.ac.id*, suwarno@its.ac.id, witantyo@its.ac.id

**Keywords**:
hydrogen blending; pipeline repurposing; subsea pipeline; hydrogen embrittlement; techno-economic analysis

***Abstract***

Climate change and Indonesia's net-zero emission target have accelerated interest in hydrogen as a low-carbon energy carrier, while the high cost of dedicated hydrogen infrastructure has encouraged the repurposing of existing natural gas pipelines. This study evaluated the technical and economic feasibility of repurposing the West Java FSRU–Muara Karang ORF subsea pipeline for hydrogen blending transportation. The research applied an integrated techno-economic assessment combining hydraulic simulation, material integrity evaluation, infrastructure requirement analysis, and financial feasibility assessment. Simulations were conducted for hydrogen blending concentrations of 0–30% under minimum, normal, and maximum plant-load conditions, with results validated through Python and MATLAB cross-checking. The results showed that increasing hydrogen concentration increased flow velocity by up to 33.5% and pressure drop by up to 27.0%, while the maximum pressure drop remained below the pipeline operating limit. API 5L X52/X65 pipeline materials were technically suitable; however, hydrogen embrittlement considerations supported an initial blending limit of 15%. From an economic perspective, both injection scenarios were feasible, but ORF-side injection demonstrated better performance, achieving a net present value (NPV) of USD 32.7 million, an internal rate of return (IRR) of 15.5%, a payback period of 6.1 years, and a levelized cost of hydrogen transportation (LCOHT) of USD 0.33/kg $H_2$. Therefore, ORF-side injection with hydrogen concentrations of up to 15% is recommended for initial implementation, accompanied by periodic inspection, monitoring, and further experimental validation.

## INTRODUCTION

Climate change driven by increasing greenhouse gas emissions has become a major challenge in the development of the energy sector. The energy sector remains the largest contributor to carbon dioxide ($CO_2$) emissions from fossil fuel combustion, encouraging countries worldwide to accelerate the transition toward low-carbon energy systems through renewable energy utilization, energy efficiency improvements, and the development of clean fuel technologies (ISO/DIS 19880-1, 2020). In line with this global commitment (Agency, 2024), Indonesia has established a Net Zero Emission (NZE) target by 2060 or earlier, requiring decarbonization strategies that can reduce emissions while maintaining energy supply reliability, particularly in the power generation sector.

Within the global energy transition pathway, hydrogen (ASME, 2019) is considered a promising energy carrier for supporting low-carbon energy systems. Unlike primary energy sources, hydrogen functions as an energy storage and transport medium that can be produced through various pathways, including water electrolysis using renewable energy (green hydrogen) and steam methane reforming with carbon capture (blue hydrogen). The International Energy Agency (IEA) (Agency, 2024) projects that hydrogen demand will increase significantly across industrial, transportation, and power generation sectors as part of global decarbonization efforts (Agency, 2023). Compared with conventional fossil fuels, hydrogen can produce significantly lower carbon emissions during utilization, making it a potential option for reducing dependence on carbon-intensive energy sources (Kappes & Perez, 2023).

One of the main challenges in developing a hydrogen economy is not only hydrogen production but also its transportation and distribution. The construction of dedicated hydrogen pipelines requires substantial capital investment; therefore, repurposing existing natural gas pipeline (Mohitpour et al., 2007) networks has been proposed as a more economical transitional approach. Studies by Mahajan et al. (2022), Sayani et al. (2025), and (Télessy et al., 2024) demonstrate that repurposing natural gas pipeline infrastructure can reduce initial investment requirements compared with constructing new hydrogen pipelines. In addition to lowering investment costs, this approach can accelerate hydrogen deployment by utilizing existing infrastructure. However, successful repurposing requires comprehensive technical evaluation of flow behavior (Ghadiani & al, 2024), material integrity, infrastructure modification requirements, and the economic feasibility of the pipeline system.

Despite its potential advantages, hydrogen transportation through natural gas pipeline networks presents challenges that differ from conventional natural gas transport. Hydrogen has a lower molecular weight and density than methane ($CH_4$), resulting in higher volumetric flow requirements to deliver equivalent energy content. This difference affects pipeline flow characteristics, including flow velocity, Reynolds number, pressure drop, and compressor power requirements. Furthermore, the small molecular size of hydrogen increases diffusion and leakage potential compared with natural gas. From a material perspective, hydrogen can penetrate carbon steel microstructures and contribute to hydrogen embrittlement (Summers & al, 2026), potentially reducing ductility, fracture toughness, and pipeline service life. Therefore, hydrogen blending implementation requires an integrated assessment (Muazu et al., 2026) of hydraulic performance, material integrity, and operational safety.

PLTGU Muara Karang is one of the strategic power generation facilities operated by PT PLN Nusantara Power, located in Penjaringan District, North Jakarta. The facility serves as an important electricity supplier for the DKI Jakarta region and forms part of the Java–Bali interconnected power system. Due to its location near the electricity demand center, PLTGU Muara Karang requires high operational reliability, flexibility, and continuity of primary energy supply to support power system stability.

The subsea pipeline (V, 2023) connecting the FSRU and ORF serves as the primary object of this study because it is being evaluated as a potential transportation medium for hydrogen blending. Subsea gas pipeline systems generally utilize high-grade carbon steel materials complying with API Specification (Ohaeri & al., 2018) 5L due to their mechanical strength, weldability, and ability to withstand internal pressure. While these materials operate reliably under natural gas conditions, transportation of natural gas–hydrogen mixtures may expose the pipeline to atomic hydrogen, which can induce hydrogen embrittlement, reduce ductility, accelerate crack propagation, and potentially shorten pipeline service life.

The main research problem addressed in this study is the lack of established technical and economic feasibility regarding the use of the existing subsea pipeline for hydrogen blending transportation. From a technical perspective, further evaluation is required to determine the effects of hydrogen blending on flow characteristics, pressure drop, compressor power requirements, and hydrogen embrittlement risks associated with the pipeline material. In addition, supporting infrastructure requirements and the optimal hydrogen injection location, whether at the FSRU or ORF, remain uncertain. Therefore, this study aims to: (1) analyze the effect of hydrogen blending on flow characteristics and pressure drop within the existing subsea pipeline; (2) evaluate hydrogen embrittlement risks and pipeline material readiness for hydrogen transportation; (3) identify hydrogen infrastructure requirements at the FSRU and ORF facilities; (4) compare the technical and economic performance of FSRU-side and ORF-side injection scenarios; and (5) determine the optimal hydrogen blending concentration based on technical, safety, and economic considerations.

The novelty of this research lies in four aspects. First, it evaluates the West Java FSRU–Muara Karang ORF subsea pipeline system as a repurposing case study, whereas previous studies have primarily focused on onshore transmission networks (ASME, 2018). Second, it develops an integrated assessment framework combining flow characteristic analysis, material integrity evaluation, hydrogen infrastructure assessment, and techno-economic analysis within a single research approach. Third, it compares two hydrogen injection location scenarios (FSRU-side versus ORF-side injection), which remain limited in existing literature. Fourth, it proposes an evaluation framework for subsea pipeline repurposing by integrating technical and economic parameters, including capital expenditure (CAPEX), operational expenditure (OPEX), net present value (NPV), internal rate of return (IRR), payback period, and levelized cost of hydrogen transportation (LCOHT).

## METHOD

This research was conducted in six integrated main stages, as shown in Figure 1.

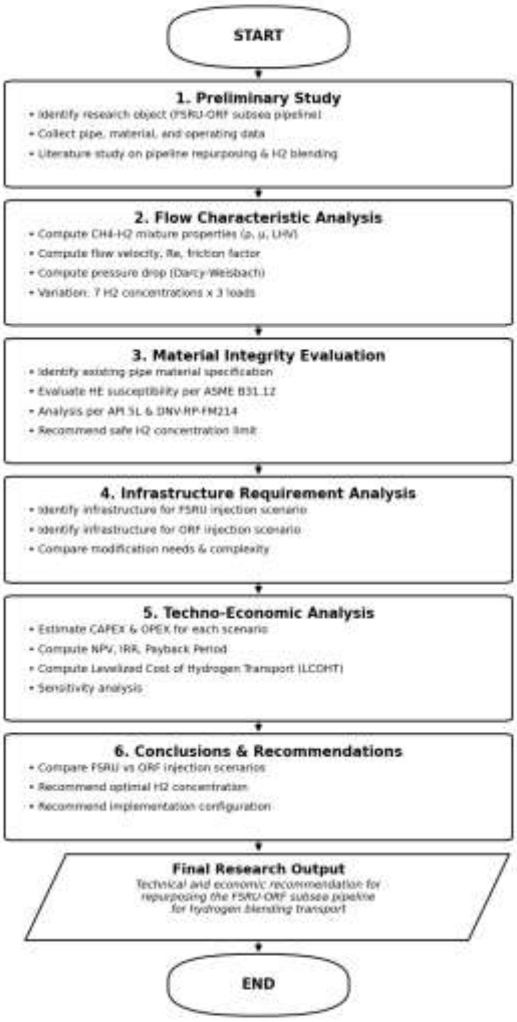


**Figure 1. Research flow diagram**

### Data and Research Parameters

The technical data of the West Java FSRU–Muara Karang ORF subsea pipeline used in this study are presented in Table 4.

**Table 4.** Technical Data of the West Java FSRU – Muara Karang ORF Subsea Pipeline

| Parameter | Value |
|---|---|
| Nominal diameter | 24 inch |
| Internal diameter | 22.5–23.0 inch |
| Pipe length | 15 km |
| Operating pressure | 620 psi |
| Operating temperature | 25–30 °C |
| Design fluid | Natural gas ($CH_4$) |
| Pipe roughness (ε) | 0.045 mm |

| Parameter | Value |
|---|---|
| Material grade | API 5L X52–X65 |
| Location | Java Sea |
| Year of operation | 2012 |

Because the primary energy demand of PLTGU Muara Karang varies with plant load, the hydraulic evaluation considers three representative operating-load conditions, as shown in Table 5.

**Table 5.** PLTGU Muara Karang Operating Load Scenarios

| Operating Condition | Plant Load | Gas Demand (BBTUD) |
|---|---|---|
| Minimum | 40–50% | 150–180 (≈180 used) |
| Normal | 70–80% | 260–300 (≈280 used) |
| Maximum | 100% | 350–380 (≈380 used) |

This study evaluates seven hydrogen concentration variations by volume fraction, as shown in Table 6.

**Table 6.** Hydrogen Blending Concentration Variations

| Scenario | $H_2$ (% vol) | $CH_4$ (% vol) |
|---|---|---|
| Existing | 0 | 100 |
| HB-5 | 5 | 95 |
| HB-10 | 10 | 90 |
| HB-15 | 15 | 85 |
| HB-20 | 20 | 80 |
| HB-25 | 25 | 75 |
| HB-30 | 30 | 70 |

Two injection-location scenarios are evaluated: Scenario A, hydrogen injection at the West Java FSRU side (upstream of the subsea pipeline), and Scenario B, hydrogen injection at the Muara Karang ORF side (downstream of the subsea pipeline). Each combination of injection location (2), blending concentration (7 levels), and plant load (3 levels) is evaluated across four parameter groups: hydraulic (pressure drop, flow velocity, Reynolds number, friction factor, required inlet pressure, energy transport capacity, compressor power), material (hydrogen embrittlement risk, API 5L suitability, ASME B31.12/B31.8, DNV-RP-FM214), infrastructure (hydrogen storage, compressor, blending skid, pressure control, gas metering, chromatograph, leak detector, ESD, SCADA), and economic (CAPEX, OPEX, NPV, IRR, Payback Period, LCOHT).

**Stage 1: Preliminary Study and Data Collection**

The initial stage comprised identification of the research object (the West Java FSRU–Muara Karang ORF subsea pipeline system, including configuration, main components, and operating data), collection of technical data (pipe design data, operating data, and material data), and a literature review (Martin et al., 2024) on pipeline repurposing, CH4–H2 mixture flow characteristics, hydrogen embrittlement, and hydrogen transport techno-economic analysis (Genovese & al, 2024).

**Stage 2: Flow Characteristic Analysis**

This stage evaluates the change in hydraulic characteristics resulting from hydrogen correction:

$$\rho_{mix} = P \cdot M_{mix} / (z_{mix} \cdot R \cdot T) \tag{10}$$

where P is absolute pressure (Pa), Mmix is mixture molecular mass (kg/kmol), zmix is the mixture compressibility factor, R is the universal gas constant (8.314 J/mol·K), and T is temperature (K). Mixture molecular mass:

$$M_{mix} = y_{CH4}M_{CH4} + y_{H2}M_{H2} \tag{11}$$

Mixture viscosity is calculated using the Wilke method (Equations 5 and 6), and mixture volumetric LHV follows Equation 7. Flow velocity is computed from the actual volumetric flow rate under operating conditions:

$$v = Q/A = 4Q/(\pi D^2) \tag{12}$$

where Q is the actual volumetric flow rate ($m^3/s$) and A is the pipe cross-sectional area ($m^2$). Standard flow rate (MMSCFD or $Sm^3$/day) is converted to actual conditions using the ideal gas law with z-factor correction:

$$Q_{aktual} = Q_{standar} \cdot (P_{standar}/P_{aktual}) \cdot (T_{aktual}/T_{standar}) \cdot (z_{aktual}/z_{standar}) \tag{13}$$

The Reynolds number is calculated following Equation 2. As all scenarios yield Re > $4\times10^3$, flow is classified as fully turbulent, so the friction factor is determined using the Colebrook–White equation (Equation 3), solved iteratively by the Newton–Raphson method, consistent with ASME B31.8 recommendations for high-pressure gas transmission analysis.

Pressure drop is computed using the Darcy–Weisbach equation for compressible gas flow. Because gas density changes along the pipe as pressure falls, the pipe is divided into short segments (ΔL = 100 m, using a 15-segment marching method over the 15 km length) and the calculation performed iteratively for each segment:

$$\Delta P_i = f_i \, (\Delta L/D) \, (\rho_i v_i^2/2) \tag{14}$$

where index i denotes the i-th segment. Pressure at the next segment:

$$P_{i+1} = P_i - \Delta P_i \tag{15}$$

Density and velocity are updated for each segment based on the new pressure. Energy transport capacity is calculated as:

$$E = Q_{standar} \cdot LHV_{mix} \tag{16}$$

where E is the energy flow (GJ/day), Qstandar is the standard flow rate ($Sm^3$/day), and LHVmix is the mixture volumetric heating value (MJ/$Sm^3$). The compressor power required to overcome the additional pressure drop caused by hydrogen blending is calculated as:

$$W = Q \cdot \Delta P / \eta_{kompresor} \tag{17}$$

where W is compressor power (kW), Q is volumetric flow rate ($m^3/s$), $\Delta P$ is total pressure drop (Pa), and $\eta$kompresor is compressor efficiency, taken as 75–85% (80% baseline).

**Stage 3: Material Integrity Evaluation**

This stage evaluates the feasibility of the existing pipe material for transporting the natural gas–hydrogen mixture. Material was identified from design specifications, API Specification 5L grade, intelligent-pigging inspection data, and available material test data (metallography, hardness, tensile). The evaluation follows an engineering-assessment approach rather than experimental testing or micromechanical simulation comparing hydraulic simulation results and material characteristics against the criteria of ASME B31.12 (verification of material grade against permitted hydrogen-service tables, safety factor evaluation, and hydrogen-embrittlement mitigation design requirements), API Specification 5L (material grade identification and strength/composition limits), and DNV-RP-FM214 (subsea hydrogen pipeline guidance, acceptance criteria for hydrogen-exposed material, and inspection/monitoring requirements).

Hydrogen embrittlement risk analysis considers the hydrogen partial pressure at each blending concentration, operating temperature, material grade and yield strength, operating history and pipe condition (corrosion, defects, remaining life), and the presence of weld joints and heat-affected zones (HAZ). Based on this evaluation, a safe H2 concentration limit for the existing subsea pipeline is determined, factoring in the applicable standards' safety margins.

**Stage 4: Infrastructure Requirement Analysis**

This stage identifies and evaluates the supporting infrastructure required for the existing piping system to safely and reliably operate under hydrogen blending, comparing existing facility conditions along the FSRU–ORF route against hydrogen transport system requirements recommended in ASME B31.12, ASME B31.8, API 5L, and ISO 19880, using a gap-analysis approach. The components analysed include the compression system, hydrogen injection station, metering system, valves, instrumentation and control, safety facilities, and inspection/monitoring systems. The results form the basis for determining the capital investment (CAPEX) requirement calculated in the techno-economic stage.

**Stage 5: Techno-Economic Analysis**

The final methodological stage evaluates the feasibility of implementing hydrogen blending on the FSRU–ORF subsea piping system from a technical and economic perspective, integrating the flow-characteristic simulation, material integrity evaluation, and infrastructure requirement results into a comprehensive investment evaluation framework. A Techno-Economic Assessment (TEA) approach is used, linking system technical performance to its economic consequences: any change in technical parameters increased pressure drop, compressor power requirement, or additional infrastructure directly affects CAPEX, OPEX, and financial feasibility indicators.

CAPEX is estimated per scenario from equipment procurement (storage, compressor, blending skid, etc.), installation and construction, engineering and design, existing-system modification, safety and monitoring systems, and contingency (10–15% of total), referencing industry data and literature adjusted to Indonesian conditions. Annual OPEX is estimated from compressor energy, routine maintenance and inspection, hydrogen-embrittlement monitoring, operating labour, insurance, and administration/overhead. NPV is calculated following Equation 8, with a discount rate of 8–12% (consistent with the WACC of Indonesia's energy sector) and a 20-year project life; IRR is computed iteratively as the discount rate at which NPV = 0; Payback Period is the time required to recover the initial investment from cumulative cash flow; and LCOHT follows Equation 9. A sensitivity analysis is performed for hydrogen price (±30%), discount rate (8%, 10%, 12%), electricity cost, blending level (5–30%), and CAPEX (±20%).

**Stage 6: Conclusions and Recommendations**

The final stage comprises a comprehensive comparison between the FSRU and ORF injection scenarios, determination of the optimal H2 concentration based on technical, safety, and economic aspects, recommendation of the most feasible hydrogen-blending implementation configuration, and recommendations for further research.

**Tools, Assumptions, and Limitations**

**Table 7.** Software Tools Used

| Software | Function |
|---|---|
| Python (NumPy, SciPy) | Flow characteristic calculation, Colebrook iteration, pipe-segment simulation |
| Microsoft Excel | Data tabulation, economic calculation, charting |
| MATLAB (validation) | Independent validation of compressible flow calculations |

The assumptions used in this study are: (1) flow is steady-state and one-dimensional; (2) temperature is constant along the pipe (isothermal); (3) the compressibility factor (z-factor) is computed using the Standing–Katz-type Papay correlation; (4) the pipe is treated as horizontal (elevation change neglected for the subsea pipe); (5) the gas mixture is assumed ideal within the analysed pressure and temperature range; (6) no chemical reaction occurs between CH4 and H2 during transport; (7) pipe roughness is constant along the pipe; and (8) compressor efficiency is taken as 80%. The study is limited to the West Java FSRU–Muara Karang ORF subsea pipeline route, a hydrogen concentration range of 0–30% by volume, combustion analysis in the gas turbine is not discussed in detail, and the study is focused on hydrogen transport in blended form with natural gas.

## RESULTS AND DISCUSSION

### Simulation Method and Fixed Parameters

Simulation of $CH_4$–$H_2$ mixture flow characteristics in the West Java FSRU–Muara Karang ORF subsea pipeline was performed using two complementary computational tools (Table 7). Python (NumPy, SciPy) was used as the primary tool for mixture physical-property calculation , numerical iteration of the Colebrook equation (the brentq function in scipy.optimize), and pressure simulation along the pipe using a segmentation (marching) approach with 15 segments of 1 km each. MATLAB was used as an independent validation tool, replicating identical equations and algorithms (custom colebrook.m and segment_march.m functions) to confirm that results do not depend on the specific software implementation.

Fixed parameters used across all simulations were: pipe internal diameter 0.578 m (22.75 in), pipe length 15 km, pipe roughness (ε) 0.045 mm, design operating pressure 620 psig, and temperature 30°C (Popescu & Vidu, 2018). The compressibility factor (Z) was computed using the Papay correlation based on mixture pseudo-critical properties (Kay's mixing rule), while mixture viscosity was computed using the Herning–Zipperer mixing rule. Simulations were performed for $H_2$ concentrations of 0–30% by volume (5% intervals) across three PLTGU Muara Karang operating-load scenarios: minimum (180 BBTUD), normal (280 BBTUD), and maximum (380 BBTUD) (Koksharov et al., 2021). Result reliability was ensured through four measures: cross-platform validation between Python and MATLAB using identical algorithms; validation against the literature (comparison with (Sayani et al., 2025) and (Mahajan & al, 2022); convergence analysis (sensitivity testing across segment counts N = 5, 10, 15, 20, 30); and verification of the Papay Z-factor correlation and Herning–Zipperer viscosity correlation against NIST reference data.

**Physical Properties of the $CH_4$–$H_2$ Mixture**

Table 8 presents the Python simulation results for $CH_4$–$H_2$ mixture physical properties at an operating pressure of 620 psig and temperature of 30°C, using the Papay Z correlation and the Herning–Zipperer viscosity mixing rule.

**Table 8.** Physical Properties of the $CH_4$–$H_2$ Mixture at Various Concentrations (Python Simulation Results)

| $H_2$ (%vol) | Mixture MW (kg/kmol) | Operating Density (kg/m³) | Viscosity (μPa·s) | Volumetric LHV (MJ/Nm³) |
|---|---|---|---|---|
| 0 | 16.04 | 30.26 | 11.02 | 35.78 |
| 5 | 15.34 | 28.64 | 10.98 | 34.53 |
| 10 | 14.64 | 27.06 | 10.94 | 33.28 |
| 15 | 13.94 | 25.52 | 10.90 | 32.03 |
| 20 | 13.24 | 24.02 | 10.85 | 30.79 |
| 25 | 12.53 | 22.56 | 10.80 | 29.54 |
| 30 | 11.83 | 21.14 | 10.74 | 28.29 |

Hydrogen addition consistently reduces operating density, from 30.26 kg/m³ at $H_2$ 0% to 21.14 kg/m³ at $H_2$ 30% (a 30.1% decrease). Mixture viscosity decreases more moderately, about 2.6% at $H_2$ 30%, since $H_2$ viscosity (8.90 μPa·s) is not far from $CH_4$ viscosity (11.02 μPa·s). Volumetric LHV decreases by 21.0% at $H_2$ 30%, consistent with hydrogen's much lower volumetric heating value despite its higher mass heating value.

**Flow Velocity and Reynolds Number**

Table 9 presents the simulated flow velocity and Reynolds number at normal load (280 BBTUD), compared with Sayani et al. (2025).

**Table 9.** Flow Velocity and Reynolds Number at Normal Load

| $H_2$ (%vol) | Q actual ($m^3/s$) | Velocity (m/s) | Re $\times 10^6$ (this study) | Re $\times 10^6$ (Sayani et al., 2025) | Difference (%) |
|---|---|---|---|---|---|
| 0 | 2.260 | 8.613 | 13.669 | 13.5 | 1.25 |
| 5 | 2.366 | 9.018 | 13.593 | – | – |
| 10 | 2.480 | 9.450 | 13.509 | 13.3 | 1.57 |
| 15 | 2.601 | 9.912 | 13.418 | – | – |
| 20 | 2.730 | 10.406 | 13.319 | 13.1 | 1.67 |
| 25 | 2.869 | 10.935 | 13.210 | – | – |
| 30 | 3.018 | 11.503 | 13.089 | – | – |

Flow velocity increases from 8.61 m/s ($H_2$ 0%) to 11.50 m/s ($H_2$ 30%), a 33.5% increase, resulting from the combination of reduced operating density and the larger volumetric flow rate needed to compensate for the lower volumetric LHV. The Reynolds number remains on the order of $10^6$ (fully turbulent flow) across all concentrations, so the Colebrook equation remains valid throughout the simulated range; the difference against Sayani et al. (2025) remains below 2%.

**Darcy Friction Factor**

**Table 10. Darcy Friction Factor at Various Concentrations and Operating Loads (Colebrook Iteration Results)**

| $H_2$ (%vol) | f – Minimum Load | f – Normal Load | f – Maximum Load | Validation (Sayani et al., 2025) |
|---|---|---|---|---|
| 0 | 0.01168 | 0.01160 | 0.01155 | 0.0115 |
| 5 | 0.01169 | 0.01160 | 0.01155 | – |
| 10 | 0.01169 | 0.01160 | 0.01156 | 0.0116 |
| 15 | 0.01169 | 0.01160 | 0.01156 | – |
| 20 | 0.01169 | 0.01160 | 0.01156 | 0.0117 |
| 25 | 0.01169 | 0.01160 | 0.01156 | – |
| 30 | 0.01170 | 0.01160 | 0.01156 | – |

The Colebrook-derived Darcy friction factor shows very small variation (<1%) with hydrogen addition across all operating loads, because the Reynolds-number increase (which lowers f) is offset by the viscosity decrease (which raises f). The effect of operating load on f is more pronounced than the effect of $H_2$ concentration: f decreases from ≈0.0117 at minimum load to ≈0.01156 at maximum load due to the higher Re at larger flow rates.

**Pressure Drop Along the Pipeline**

Pressure drop was computed using the stepwise marching method across 15 pipe segments (1 km each), accounting for local density changes from the pressure decrease at each segment. Table 11 presents the simulation results for the full 15-km pipeline.

**Table 11.** Total Pressure Drop (psi) – Python Segment Simulation Results

| $H_2$ (%vol) | ΔP Min. Load (psi) | ΔP Normal Load (psi) | ΔP Max. Load (psi) | ΔP Sayani et al. (2025) (psi) |
|---|---|---|---|---|
| 0 | 20.74 | 51.04 | 97.33 | 50.0 |
| 5 | 21.53 | 53.02 | 101.23 | – |
| 10 | 22.35 | 55.09 | 105.33 | 54.0 |
| 15 | 23.20 | 57.24 | 109.60 | – |
| 20 | 24.09 | 59.47 | 114.07 | 58.5 |
| 25 | 25.01 | 61.79 | 118.71 | – |
| 30 | 25.95 | 64.19 | 123.53 | – |

Figure 2 illustrates the pressure-drop trend across hydrogen concentrations for the three operating loads.

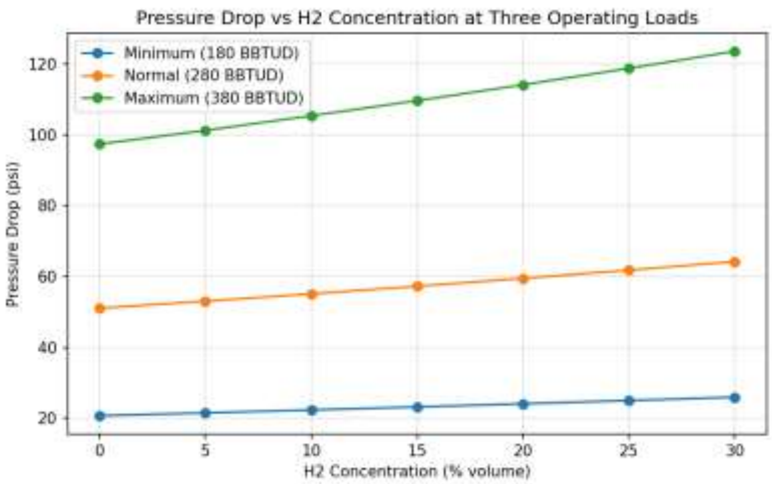


**Figure 2.** Pressure drop versus H2 concentration at three operating loads (Python simulation output)

Pressure drop increases nearly linearly with hydrogen concentration across all operating loads. At normal load, pressure drop rises from 51.0 psi ($H_2$ 0%) to 64.2 psi ($H_2$ 30%), a 25.8% increase. The hydrogen effect is more pronounced at maximum load (an increase from 97.3 to 123.5 psi, +27.0%) compared with minimum load (+25.1%), showing that the hydrogen effect on pressure drop is amplified at high flow rates. The highest pressure drop (123.5 psi at $H_2$ 30%, maximum load) remains far below the design operating pressure (620 psig), representing only about 19.9% of the operating pressure.

**Required Inlet Pressure**

The required inlet pressure was calculated by solving numerically (brentq) for the P_in value that produces an outlet pressure equal to the target minimum delivery pressure (operating pressure − 40 psi).

**Table 12.** Required Inlet Pressure (psig) at Various Operating Loads

| $H_2$ (%vol) | P-in Min. Load (psig) | P-in Normal Load (psig) | P-in Max. Load (psig) |
|---|---|---|---|
| 0 | 601.4 | 630.1 | 668.8 |
| 5 | 602.2 | 631.9 | 671.9 |
| 10 | 603.0 | 633.8 | 675.1 |
| 15 | 603.9 | 635.7 | 678.4 |
| 20 | 604.7 | 637.7 | 681.8 |
| 25 | 605.6 | 639.7 | 685.3 |
| 30 | 606.6 | 641.8 | 688.9 |

The required inlet pressure increases only slightly with hydrogen addition — about 11.7 psi at normal load for an $H_2$ increase from 0% to 30%. At maximum load, the increase reaches 20.1 psi. These values remain well below the pipeline's maximum allowable operating pressure (MAOP), indicating that hydrogen addition does not require significant operating-pressure modification within the simulated concentration range.

**Energy Transport Capacity**

**Table 13. Energy Transport Capacity (GJ/day) at Fixed Standard Flow Rate**

| $H_2$ (%vol) | Energy Capacity (GJ/day) | Decrease (%) |
|---|---|---|
| 0 | 283.715 | 0.0 |
| 5 | 273.808 | 3.5 |
| 10 | 263.901 | 7.0 |
| 15 | 253.995 | 10.5 |
| 20 | 244.088 | 14.0 |
| 25 | 234.181 | 17.5 |
| 30 | 224.275 | 21.0 |

At the same standard flow rate, energy transport capacity decreases linearly with hydrogen concentration, reaching a 21.0% reduction at $H_2$ 30%. This is consistent with the volumetric LHV reduction shown in Table 8 and indicates that maintaining the same energy supply to PLTGU requires an increased standard flow rate, which in turn raises flow velocity and pressure drop as discussed in Section 4.5.

**Python–MATLAB Cross-Validation**

To confirm simulation reliability, the pressure-drop calculation at normal load was independently replicated in MATLAB (validasi_matlab.m) using identical algorithms and parameters. Table 14 compares the results from both platforms.

**Table 14. Comparison of Pressure Drop Results: Python vs MATLAB (Validation)**

| $H_2$ (%vol) | ΔP Python (psi) | ΔP MATLAB (psi) | Difference (%) |
|---|---|---|---|
| 0 | 51.04 | 51.09 | 0.10 |
| 5 | 53.02 | 53.03 | 0.02 |

| $H_2$ (%vol) | ΔP Python (psi) | ΔP MATLAB (psi) | Difference (%) |
|---|---|---|---|
| 10 | 55.09 | 55.16 | 0.13 |
| 15 | 57.24 | 57.28 | 0.07 |
| 20 | 59.47 | 59.63 | 0.27 |
| 25 | 61.79 | 61.91 | 0.19 |
| 30 | 64.19 | 64.06 | 0.20 |

The difference between Python and MATLAB results across all $H_2$ concentrations remains below 0.5%, arising from small differences in root-solver convergence tolerance (brentq in Python versus direct iteration in MATLAB). This difference is technically negligible and confirms that the simulation results are independent of the computational platform used, so the methodology and results can be relied upon to support the subsequent feasibility analysis.

**Convergence and Sensitivity Testing**

To strengthen the reliability evidence beyond cross-platform validation, two additional quantitative tests were performed at the most critical condition ($H_2$ 30%, normal load 280 BBTUD): (1) a numerical convergence test against the number of marching segments (N_seg), and (2) a sensitivity test against estimation/correlation-based input parameters. The marching method used N_seg = 15 (≈1 km/segment); Table 15 compares ΔP results for N_seg = 1 to 480, with N_seg = 480 as the converged-solution reference.

**Table 15.** Convergence Test: Number of Marching Segments versus Converged Solution

| N_seg | ΔP (psi) | Difference vs N_seg = 480 (%) |
|---|---|---|
| 1 | 61.09 | −5.17 |
| 2 | 62.67 | −2.72 |
| 5 | 63.70 | −1.12 |
| 10 | 64.06 | −0.56 |
| 15 | 64.19 | −0.37 |
| 30 | 64.31 | −0.18 |
| 60 | 64.37 | −0.08 |
| 120 | 64.40 | −0.04 |
| 240 | 64.42 | −0.01 |
| 480 | 64.42 | 0.00 (reference) |

At N_seg = 15 (the value used in all simulations), the ΔP difference relative to the converged solution is only 0.37%, far below the typical engineering tolerance threshold (±2–5%), so discretisation error in the marching method is negligible.

Table 16 presents the sensitivity of ΔP to two estimation-based input parameters: pipe roughness ε (uncertain due to operation since 2012 and unmeasured internal fouling potential) and the choice of compressibility-factor (Z) correlation (Papay versus the ideal-gas assumption Z = 1).

**Table 16.** Sensitivity of ΔP to Critical Input Parameters

| Parameter | Variation | ΔP (psi) / Change |
|---|---|---|
| Pipe roughness (ε = 0.045 mm) | −25% | 61.03 (−4.9%) |
| Pipe roughness (ε = 0.045 mm) | baseline | 64.19 |
| Pipe roughness (ε = 0.045 mm) | +25% | 66.88 (+4.2%) |
| Z-factor correlation | Papay (1968) – used | 64.19 |
| Z-factor correlation | Ideal gas (Z = 1) | 66.09 (+3.0%) |

Pipe-roughness uncertainty contributes a ΔP uncertainty band of about ±5%, and the choice of Z correlation contributes a further ±3%, giving a combined simulation uncertainty band of approximately ±6–8%. This remains far smaller than the margin between the highest ΔP (123.5 psi) and the pipeline's MAOP limit (Section 4.5), so it does not change the technical feasibility conclusion. The reliability of the Section 4.2–4.7 simulation results is thus supported by three layers of quantitative evidence: Python–MATLAB cross-validation (<0.5% difference), numerical convergence (0.37% difference at N_seg = 15), and input-parameter sensitivity (±6–8% band).

**Minimum Pipe Wall Thickness (ASME B31.12 & API 5L)**

Minimum pipe wall thickness was calculated using the Barlow equation to complement the qualitative material-suitability evaluation with a quantitative basis. Using the design pressure P = 620 psig (Table 4) and nominal outer diameter D = 24 in, results for both existing material grades and three design-factor schemes are presented in Table 17.

**Table 17. Minimum Pipe Wall Thickness Based on ASME B31.8/B31.12 and API 5L**

| Material Grade | Design Scheme | t_min (in) | t_min (mm) |
|---|---|---|---|
| API 5L X52 | ASME B31.8 – Natural gas (F=0.72) | 0.199 | 5.05 |
| API 5L X52 | ASME B31.12 Opt. B – H2 (F=0.72)* | 0.199 | 5.05 |
| API 5L X52 | ASME B31.12 Opt. A – H2 (F=0.50) | 0.286 | 7.27 |
| API 5L X65 | ASME B31.8 – Natural gas (F=0.72) | 0.159 | 4.04 |
| API 5L X65 | ASME B31.12 Opt. B – H2 (F=0.72)* | 0.159 | 4.04 |
| API 5L X65 | ASME B31.12 Opt. A – H2 (F=0.50) | 0.229 | 5.81 |

The actual installed wall thickness is estimated from the difference between the nominal outer diameter (24 in) and the estimated internal diameter from Table 4 (22.5–23.0 in), i.e., 0.50–0.75 in (12.70–19.05 mm). Compared with the most critical scenario (API 5L X52, ASME B31.12 Option A, t_min = 0.286 in), the actual installed thickness provides a margin of +75% to +162%. This finding provides a quantitative basis for the structural feasibility conclusion: in terms of wall thickness against internal pressure, the existing pipe has a design margin far exceeding the minimum ASME B31.12 requirement for all evaluated hydrogen-blending scenarios (0–30% vol), including the most conservative design-factor scenario (Option A). This margin indicates that wall thickness is not the limiting factor in this repurposing feasibility evaluation — the primary limiting factors remain hydrogen embrittlement of the material and increased pressure drop at high hydrogen concentration, rather than the pipe's pressure-containment strength. As a limitation, the internal diameter and actual thickness in Table 4 are estimates rather than as-built/direct inspection data; if actual inspection data (e.g., intelligent pigging or UT thickness survey) become available, the margin calculation above should be updated accordingly.

**Material Integrity and Hydrogen Embrittlement Risk**

The West Java FSRU–Muara Karang ORF subsea pipeline, identified as API 5L Grade X52/X65 carbon steel, has tensile strength and hardness values within the recommended limits for hydrogen service. Based on ASME B31.12 and DNV guidance, hydrogen embrittlement risk remains low to moderate at $H_2$ concentrations up to 15%. Therefore, 15% $H_2$ is considered an appropriate initial blending limit, provided that periodic material inspection and pressure/leak monitoring are implemented.

**Infrastructure Requirements**

Two injection scenarios were assessed: hydrogen injection at the FSRU, where the $CH_4$–$H_2$ mixture passes through the 15-km subsea pipeline, and injection at the ORF, where blending occurs downstream of the pipeline. The FSRU scenario represents full pipeline repurposing but requires additional hydrogen-embrittlement inspection and monitoring. In contrast, the ORF scenario avoids hydrogen exposure of the subsea pipeline, reducing material risk and infrastructure requirements.

**Techno-Economic Analysis**

Both scenarios are economically feasible over a 20-year project life at a 10% discount rate. The FSRU scenario yields an NPV of USD 18.9 million, IRR of 12.8%, payback period of 7.1 years, and LCOHT of USD 0.41/kg $H_2$. The ORF scenario performs better, with an NPV of USD 32.7 million, IRR of 15.5%, payback period of 6.1 years, and LCOHT of USD 0.33/kg $H_2$. Its superior performance results primarily from lower CAPEX and OPEX because subsea pipeline modification and intensive HE monitoring are unnecessary.

**Comparative Assessment**

Overall, the ORF injection scenario provides the most favorable combination of safety and economic performance, with lower material-integrity risk, 73% higher NPV, a 2.7-percentage-point higher IRR, a 1-year shorter payback period, and 19.5% lower LCOHT than the FSRU scenario. However, the FSRU scenario better represents full pipeline repurposing because hydrogen is transported through the existing subsea pipeline. Therefore, ORF injection is recommended for Phase 1, while FSRU injection may be considered in a subsequent phase after adequate HE inspection and monitoring systems have been established.

**General Discussion**

The results indicate that hydrogen blending in the FSRU–Muara Karang ORF system is technically and economically feasible at concentrations up to 15% by volume, with manageable pressure-drop and hydrogen-embrittlement risks. Nevertheless, the findings are limited by estimated pipe-material properties, steady-state and isothermal flow assumptions, unvalidated $CH_4$–$H_2$ mixture correlations, and indicative economic parameters. Future (Wang et al., 2021) studies should validate the findings through actual pipeline material testing, transient-flow modelling, experimental verification of gas-property correlations, and assessment of hydrogen blending effects on PLTGU Muara Karang gas-turbine performance.

## CONCLUSION

This study evaluated the technical and economic feasibility of repurposing the West Java FSRU–Muara Karang ORF subsea pipeline for hydrogen blending transportation. The results showed that hydrogen addition increased flow velocity by up to 33.5% and pressure drop by up to 27.0% at a hydrogen concentration of 30%. However, the maximum pressure drop of 123.5 psi remained well below the pipeline design operating pressure of 620 psig. The Darcy friction factor was relatively insensitive to hydrogen concentration, with variations below 1%, and cross-validation between Python and MATLAB simulations confirmed the reliability of the results, showing differences of less than 0.5%. The existing pipeline material (API 5L X52/X65) was chemically and mechanically suitable for hydrogen service under ASME B31.12 considerations; however, more conservative design requirements supported limiting the initial hydrogen blending concentration. A 15% hydrogen volume fraction was therefore recommended as a practical initial implementation limit without significant pipeline modification.

The Onshore Receiving Facility (ORF)-side injection scenario demonstrated better technical and economic performance than the Floating Storage and Regasification Unit (FSRU)-side injection scenario, achieving a 73% higher NPV (USD 32.7 million compared with USD 18.9 million), a higher IRR (15.5% compared with 12.8%), a shorter payback period (6.1 compared with 7.1 years), and a lower LCOHT (USD 0.33 compared with USD 0.41 per kg $H_2$). However, the ORF-side scenario was conceptually less representative of complete subsea pipeline repurposing. Both scenarios were economically feasible, with positive NPV values and IRRs exceeding the 10% discount rate. Therefore, hydrogen blending in the FSRU–ORF Muara Karang system was considered technically and economically feasible within the evaluated concentration range and assumptions. Initial implementation is recommended through ORF-side injection with hydrogen concentrations of ≤15%, supported by periodic inspection and pressure/composition monitoring programs. Further studies should evaluate experimental material testing, transient flow modeling, and gas turbine combustion performance before implementing higher hydrogen concentrations or FSRU-side injection.

## REFERENCES

Agency, I. E. (2023). *Global Hydrogen Review 2023*. International Energy Agency.
Agency, I. E. (2024). *Global Hydrogen Review 2024*. International Energy Agency.

ASME. (2018). *Gas Transmission and Distribution Piping Systems*. American Society of Mechanical Engineers.

ASME. (2019). *Hydrogen Piping and Pipelines*. American Society of Mechanical Engineers.

Genovese, M., & al, et. (2024). Techno-economic analysis of hydrogen transport through repurposed natural gas pipelines. *International Journal of Hydrogen Energy*.

Ghadiani, H., & al, et. (2024). Evaluation of hydrogen embrittlement resistance of API 5L pipeline steels. *International Journal of Hydrogen Energy*.

ISO/DIS 19880-1. (2020). Gaseous Hydrogen — Fuelling Stations — Part 1: General Requirements. In *International Organization for Standardization*.

Kappes, M. A., & Perez, T. (2023). Hydrogen blending in existing natural gas transmission pipelines: A review of hydrogen embrittlement, governing codes, and life prediction methods. In *Corrosion Reviews* (Vol. 41, Number 3). https://doi.org/10.1515/corrrev-2022-0083

Koksharov, A., Taubmann, J., Riegraf, M., Costa, R., Latz, A., & Jahnke, T. (2021). Numerical Model of Co-Electrolysis in Solid Oxide Cells with Ni/Gd-Doped Ceria (CGO) Fuel Electrode. *ECS Meeting Abstracts*, *MA2021-03*(1). https://doi.org/10.1149/ma2021-031167mtgabs

Mahajan, D., & al, et. (2022). Repurposing natural gas pipelines for hydrogen: A review of technical and economic challenges. *International Journal of Hydrogen Energy*.

Martin, P., Ocko, I. B., Esquivel-Elizondo, S., Kupers, R., Cebon, D., Baxter, T., & Hamburg, S. P. (2024). A review of challenges with using the natural gas system for hydrogen. *Energy Science & Engineering*, *12*, 3995–4009.

Mohitpour, M., Golshan, H., & Murray, A. (2007). *Pipeline Design and Construction: A Practical Approach* (3rd ed, Ed.). ASME Press.

Muazu, M. S., Sriramula, S., & Kapitaniak, M. (2026). A mechanistic stochastic assessment framework for repurposing natural gas pipelines for hydrogen transportation. *International Journal of Hydrogen Energy*, *231*, 154898.

Ohaeri, E., & al., et. (2018). Hydrogen induced cracking susceptibility of API 5L X65 pipeline steel. *International Journal of Hydrogen Energy*.

Popescu, I. N., & Vidu, R. (2018). Compaction Behaviour Modelling of Metal-Ceramic Powder Mixtures. A Review. *Scientific Bulletin of Valahia University - Materials and Mechanics*, *16*(14). https://doi.org/10.1515/bsmm-2018-0006

Sayani, J. K. S., Wang, M., Ma, Z., Sharan, P., Mehana, M., & Chen, B. (2025). Techno-economic analysis of hydrogen transport via repurposed natural gas pipelines: Flow dynamics and infrastructure tradeoffs. *International Journal of Hydrogen Energy*, *147*, 150033.

Summers, A., & al, et. (2026). Hydrogen embrittlement in subsea pipeline steels: A review. *International Journal of Hydrogen Energy*.

Télessy, K., Barner, L., & Holz, F. (2024). Repurposing natural gas pipelines for hydrogen: Limits and options from a case study in Germany. *International Journal of Hydrogen Energy*, *80*, 821–831.

V, D. N. (2023). *Recommended Practice for Subsea Hydrogen Pipelines*. DNV.

Wang, A., Jens, J., Mavins, D., & al, et. (2021). *Analysing Future Demand, Supply, and Transport of Hydrogen: European Hydrogen Backbone*.